NIH Public Access
Author Manuscript
Neuroimage. Author manuscript; available in PMC 2015 December 01.

Published in final edited form as:
Neuroimage. 2014 December ; 103: 533–541. doi:10.1016/j.neuroimage.2014.08.025.

Three-dimensional Acquisition of Cerebral Blood Volume and Flow Responses during Functional Stimulation in a Single Scan

Ying Cheng[1,2], **Peter C. M. van Zijl**[1,3], **James J. Pekar**[1,3], and **Jun Hua**[1,3,*]

[1]Division of MR Research, Russell H. Morgan Department of Radiology and Radiological Science, Johns Hopkins University School of Medicine, Baltimore, MD, USA

[2]Department of Biomedical Engineering, Johns Hopkins University School of Medicine, Baltimore, MD, USA

[3]F. M. Kirby Research Center for Functional Brain Imaging, Kennedy Krieger Institute, Baltimore, MD, USA

Abstract

In addition to the BOLD scan, quantitative functional MRI studies require measurement of both cerebral blood volume (CBV) and flow (CBF) dynamics. The ability to detect CBV and CBF responses in a single additional scan would shorten the total scan time and reduce temporal variations. Several approaches for simultaneous CBV and CBF measurement during functional MRI experiments have been proposed in two-dimensional (2D) mode covering one to three slices in one repetition time (TR). Here, we extended the principles from previous work and present a three-dimensional (3D) whole-brain MRI approach that combines the vascular-space-occupancy (VASO) and flow-sensitive alternating inversion recovery (FAIR) arterial spin labeling (ASL) techniques, allowing the measurement of CBV and CBF dynamics, respectively, in a single scan. 3D acquisitions are complicated for such a scan combination as the time to null blood signal during a steady state needs to be known. We estimated this using Bloch simulations and demonstrate that the resulting 3D acquisition can detect activation patterns and relative signal changes of quality comparable to that of the original separate scans. The same was found for temporal signal-to-noise ratio (SNR) and contrast-to-noise ratio (CNR). This approach provides improved acquisition efficiency when both CBV and CBF responses need to be monitored during a functional task.

Keywords

VASO; vascular-space-occupancy; ASL; arterial spin labeling; FAIR; flow-sensitive alternating inversion recovery; three-dimensional; whole-brain; CBV; CBF; fMRI

© 2014 Elsevier Inc. All rights reserved.

Corresponding Author: Jun Hua, Ph.D., Johns Hopkins University School of Medicine, Department of Radiology, Kennedy Krieger Institute, F.M. Kirby Research Center for Functional Brain Imaging, 707 N Broadway, Baltimore, MD, 21205, jhua@mri.jhu.edu, Tel: 443-923-9551, Fax: 443-923-9505.

Publisher's Disclaimer: This is a PDF file of an unedited manuscript that has been accepted for publication. As a service to our customers we are providing this early version of the manuscript. The manuscript will undergo copyediting, typesetting, and review of the resulting proof before it is published in its final citable form. Please note that during the production process errors may be discovered which could affect the content, and all legal disclaimers that apply to the journal pertain.

NIH-PA Author Manuscript
NIH-PA Author Manuscript
NIH-PA Author Manuscript

NIH-PA Author Manuscript

NIH-PA Author Manuscript

NIH-PA Author Manuscript

Introduction

Cerebral blood volume (CBV) and cerebral blood flow (CBF) are two fundamental parameters in brain physiology. For instance, CBV and CBF responses during functional stimulation are required to quantify cerebral metabolic rate of oxygen (CMRO2) dynamics in most quantitative blood-oxygenation-level-dependent (BOLD) approaches, such as the calibrated BOLD approach (Blockley et al., 2013; Davis et al., 1998; Hoge et al., 1999; Lin et al., 2008, 2009; Lin et al., 2011) and other models (Donahue et al., 2009a; Hua et al., 2011c; Huber et al., 2013; Lin et al., 2008, 2009; Lin et al., 2011; Lu et al., 2004b; Uh et al., 2011). In the calibrated BOLD method, CMRO2 change is estimated from BOLD and CBF changes measured during separate vascular and neuronal tasks, where the vascular stimulation is used as the calibration condition for BOLD signals. A different BOLD model proposed by Lu and van Zijl (Lu et al., 2004b), and later used and refined by others, estimates CMRO2 change from separately measured BOLD, CBF and CBV responses during neuronal tasks (no vascular task is involved in this model). Accurate information about CBF and CBV dynamics is critical in both models. In the calibrated BOLD method, the CBV change is often derived from the measured CBF change using Grubb's equation with a constant exponent (Grubb et al., 1974), which is commonly assumed to be identical in vascular and neuronal tasks. However, recent studies have shown that this power-law relationship between CBF and CBV can vary substantially under different conditions (Blockley et al., 2009; Chen and Pike, 2009; Donahue et al., 2009d; Hua et al., 2010; Hua et al., 2011c; Ito et al., 2001; Lin et al., 2008; Rostrup et al., 2005). (Lin et al., 2008) demonstrated that using dynamic CBV measurements improves the accuracy for estimating $CMRO_2$ changes during functional stimulations, as compared with calculating CBV changes from CBF measurements and the Grubb's equation with an assumed constant. Therefore, it is important to measure both CBV and CBF dynamics to capture microvascular status alterations during functional stimulations.

The ability to detect CBV and CBF responses in one single scan is desirable as it will not only shorten total scan duration, but also reduce temporal variation due to factors such as subject motion, task performance, and physiologic changes between scans. The arterial spin labeling (ASL) technique can be used to measure CBF and CBV changes in the same scan by acquiring images at multiple post-labeling delays(Alsop et al., 2014; Brookes et al., 2007; Donahue et al., 2006b; Francis et al., 2008). However, the scan time of this method is relatively long compared to the typical temporal resolution in functional studies. A number of MRI methods have been developed to measure CBV or CBF *separately*. For instance, CBV and CBF changes can be *separately* measured with vascular-space-occupancy (VASO) MRI (Lu et al., 2003) and flow-sensitive alternating inversion recovery (FAIR) arterial spin labeling (ASL) MRI (Kim, 1995; Kwong et al., 1995), respectively. Based on the T1 difference between blood and brain tissue, VASO MRI employs a spatially nonselective inversion pulse to invert both blood and tissue signals and acquires MR images at the time when blood signal recovers to zero (nulled), which can be used to calculate CBV changes (Lu et al., 2003). In FAIR ASL, an inversion pulse with and without spatially selective gradient is applied to produce the tagged and control images, respectively, from which CBF maps can be deduced (Kim, 1995; Kwong et al., 1995). Thus, a common feature in the pulse

NIH-PA Author Manuscript

NIH-PA Author Manuscript

NIH-PA Author Manuscript

sequences of both methods is that an inversion pulse is exploited to perturb the blood water spins before image acquisition. The major difference, on the other hand, is that VASO images are always acquired at the blood nulling inversion time (TI), while FAIR ASL images need to be acquired at a much longer post-labeling delay (TI≈1.5–2s) (Alsop and Detre, 1996; Donahue et al., 2006a; Silva et al., 1997; Ye et al., 1997) to allow water exchange in the capillary bed to take place. Therefore, it is possible to combine VASO and FAIR MRI to share the same inversion pulse and acquire CBV and CBF weighted images at two different TIs in a single scan. Based on this principle, (Yang et al., 2004) previously devised an elegant technique for concurrent measurement of CBV, CBF and BOLD responses during functional stimulation. This method has recently been implemented on a 7T human MRI scanner by (Krieger et al., 2013). Another method for simultaneous measurement of CBV and CBF is the double-echo FAIR (DEFAIR) approach proposed by (Thomas et al., 2001), in which CBF is measured with FAIR ASL and CBV is determined based on the different T_2 values calculated from the double echoes in the intra- and extravascular compartments. Both techniques were implemented in two-dimensional (2D) mode to acquire a single slice (Lin et al., 2008, 2009; Lin et al., 2011; Yang et al., 2004) or three slices (Gu et al., 2005) in one repetition time (TR).

Here, we propose a 3D MRI approach to measure CBV and CBF responses during functional stimulation in one single scan. It exploits the same principle as (Yang et al., 2004), which combines VASO and FAIR MRI with a common inversion pulse. A single-shot 3D fast gradient echo (GRE, also known as turbo field echo, TFE or TurboFLASH) sequence was used for image acquisition at two TIs. In addition, the magnetization pathways were simulated. The 3D VASO-FAIR sequence was implemented on a 3T human MRI scanner, and functional experiments with visual stimulation were performed on healthy volunteers to compare the data of the combined sequence and original separate scans in order to validate accuracy of the combined scan.

Materials and Methods

Pulse Sequence and Simulations

Figure 1 illustrates the combined 3D VASO-FAIR pulse sequence. Similar to the FAIR sequence, interleaving slab-selective (SS) and non-selective (NS) inversion preparation were employed. In each of the SS and NS scans, two image acquisition modules are deployed after the inversion at different TIs: TI_1 (blood nulling) and TI_2. CBV-weighted VASO images are obtained at TI_1 after NS inversion when the blood signal is nulled, and FAIR images are collected at a later time TI_2 in both SS and NS scans. These two FAIR components are combined later to obtain the CBF-weighted signals. A single-shot 3D fast GRE sequence with centric (low-high) phase encoding profile was employed in all imaging modules. This readout has recently been used in VASO MRI, which showed minimal geometrical distortion and signal dropouts, low power deposition due to small flip angles, and negligible T_2^* contamination in VASO fMRI because of the very short echo time (TE) used (Hua et al., 2013a).

A magnetization transfer (MT) prepulse was applied immediately before the inversion pulses to prepare a smaller tissue magnetization, thus expediting the inversion recovery

NIH-PA Author Manuscript NIH-PA Author Manuscript NIH-PA Author Manuscript

process so that the detectable tissue signals, and thus their signal-to-noise ratios (SNRs) are enhanced (Hua et al., 2009a; Hua et al., 2013a). When using moderate irradiation power and durations, and a frequency offset sufficiently far away from water resonance (40ppm or more), the MT prepulse has been shown to have negligible effect on blood signal so that the same blood nulling TI can be used for VASO(Balaban et al., 1991; Hua et al., 2009a; Hua et al., 2013a; Wolff and Balaban, 1989)

A spatially nonselective saturation (90° RF pulse followed by spoiler gradients) was deployed immediately after the second imaging module to set all residual magnetization (blood and tissue) to zero. The purpose for this post-saturation module is two-fold. First, it suppresses the inflow effect due to non-steady-state blood spins in VASO MRI by establishing a steady state for all blood spins entering the RF transmit coil after the first repetition time (TR) (Hua et al., 2013a; Lu, 2008; Wu et al., 2007a). Second, it ensures that blood spins in and outside the inversion slab applied in the SS scan will have the same steady-state blood nulling condition in the following NS scan. This is illustrated with Bloch simulations in Figure 2. Signal evolution during the 3D fast GRE readout was calculated using the same imaging parameters described in Experiments. Typical T_1 and T_2 values for blood, gray matter (GM), white matter (WM) and cerebrospinal fluid (CSF) in healthy human brain at 3T were used: $T_{1,blood}$ = 1624ms (Lu et al., 2004a), $T_{1,GM}$ = 1122ms (Lu et al., 2005), $T_{1,WM}$ = 758ms (Lu et al., 2005), $T_{1,CSF}$ = 3817ms (Lu et al., 2005), $T_{2,GM}$ = 80ms (Lu et al., 2005), $T_{2,WM}$ = 80ms (Lu et al., 2005), $T_{2,blood}$ = 55ms (Zhao et al., 2007), $T_{2,CSF}$ = 1442ms (Donahue et al., 2006a). The establishment of a steady state after the first TR with the post-saturation module applied immediately after the second readout, is illustrated in Figure 2a. For VASO, after the first pair of NS and SS scans, both blood in and outside the SS inversion slab will always have the same blood nulling time in the following NS scans, so that potential complications from inflowing blood are eliminated. For FAIR ASL, in-slab blood signals are identical at TI_2 in both NS and SS scans, which minimizes its contamination to the CBF measurement. On the other hand, signal from blood outside the inversion slab is higher at TI_2 in the SS scans, which is used to deduce CBF information upon subtraction of the NS and SS scans. Without the post-saturation module (Figure 2b), a steady state is not reached until the fourth TR in the simulations. Furthermore, even when this steady state is reached, the out-of-slab blood signal in VASO is still not properly nulled at TI_1 (Figure 2b inset), because the blood nulling times are different for in-slab and out-of-slab blood without the post-saturation module (effective TR is different). In-slab blood signals in the FAIR scans are still identical at TI_2 in both NS and SS scans during steady state.

The same simulations were used to estimate blood nulling TIs in VASO scans and to evaluate GM and CSF signals. A 20% signal drop after the MT saturation pulse were assumed for GM (typical values under similar saturation schemes (Hua et al., 2009a)), and no MT effect for CSF. The steady state GM signals from the simulations were 23% (of the equilibrium signal) (separate) and 20% (combined) in the VASO scans, and 59% (separate) and 57% (combined) in the FAIR scans. The steady state CSF signals were −9% (separate) and −4% (combined) in the VASO scans, and 15% (separate) and 19% (combined) in the FAIR scans. Assuming a 30% increase of CBV upon activation, the relative VASO signal change from the simulations is −1.87% in a pure GM voxel for both separate and combined

NIH-PA Author Manuscript

NIH-PA Author Manuscript

NIH-PA Author Manuscript

VASO scans, and is −1.90% (VASO in combined scan) and −1.92% (separate VASO scan) in a voxel with 5% CSF and 95% GM in volume.

Experiments

The protocol was approved by the Johns Hopkins Medicine Institutional Review Board. Subjects gave written informed consent before participating. Experiments were performed on a 3T human MRI scanner (Philips Healthcare, Best, The Netherlands), using a body coil for RF transmission and a 32-channel head coil for reception. Six healthy volunteers were scanned for this study. Three fMRI experiments with visual stimulation (yellow/blue flashing checkerboard, 24s visual stimulation interleaved with 42s cross-hair fixation, repeated 4 times) were performed on each participant: (a) 3D VASO-FAIR (TR/TI_1/TI_2=3/0.552/1.552s). A 400ms 2.5μT block-shaped MT prepulse with a frequency offset at −40 ppm (Hua et al., 2013a) was applied immediately before the inversion pulses in both NS and SS scans. (b) VASO (TR/TI = 3/0.743s). The same MT prepulse and post-saturation module as in 3D VASO-FAIR were applied. (c) FAIR (TR/TI = 3/1.552s). The order of the experiments was counterbalanced across participants. Bloch simulations (described above) were performed to estimate steady state blood nulling times for VASO scans in order to account for the influence from the 3D fast GRE readout and the post-saturation module. Note that TI_1 in the combined 3D VASO-FAIR sequence is different from TI in VASO because of the different numbers of readouts, corresponding to different recovery times after the post-saturation module (before next inversion) in the two sequences (thus different steady states). Although this leads to different inflow times (TI) for VASO, it should not have a major influence on the VASO signals if the inflow effect (see Discussion) is largely suppressed by the post-saturation module. Frequency offset corrected inversion (FOCI) pulses (Ordidge et al., 1996) were used for inversion in all scans, which are expected to produce sharper edges for spatially selective inversion than hyperbolic secant (HS) pulses (Hua et al., 2011a; Hua et al., 2011b). Common imaging parameters: voxel size = 5mm isotropic, 16 slices, field of view (FOV) = 192×192 mm^2, TR_{GRE} (TR between two consecutive echoes in 3D GRE)/TE = 3.6/1.6ms, flip angle = 7°, turbo direction = radial, parallel imaging (SENSE) acceleration factor = 3×2 (APxFH), no partial Fourier sampling, readout duration for one image volume = 391 ms. Based on the thickness of the imaging volume (80mm), the thickness of the SS inversion slab was chosen to be 100 mm.

Data Processing

The Statistical Parametric Mapping (SPM 8, University College London, UK) software package and several in-house Matlab R2012a (Mathworks, Natick, MA, USA) routines were used for data analysis. All fMRI images were corrected for motion and baseline drift. CBF-weighted images were obtained using a surround subtraction method, in which the SS/NS FAIR ASL images are subtracted with linear interpolation between the surrounding NS/SS images, respectively (Lu et al., 2006). A general linear model (GLM) was used to detect activated voxels ($P < 0.01$, t-score ≤ −1.5 for VASO and t-score ≥ 1.5 for FAIR). A SNR threshold of 20 for VASO images was used(Donahue et al., 2006b). Due to the low SNR in the subtracted FAIR ASL images, a SNR threshold of 1 was used. The relative signal change (ΔS/S) in each voxel was quantified as the difference between average signals during the baseline and activation periods normalized by the average baseline signal. In order to avoid

NIH-PA Author Manuscript

NIH-PA Author Manuscript

NIH-PA Author Manuscript

the transitional periods when calculating average signals, images acquired during the first 18s and 6s during the baseline and activation periods, respectively, were excluded. Temporal SNR (tSNR) was calculated as the voxel-wise average baseline signal divided by the standard deviation along the time course during the baseline period. Contrast-to-noise ratio (CNR) per scan was defined as the product of absolute value of relative signal change (ΔS/S) and tSNR. CNR per unit time was taken as the product of CNR per scan and square root of number of image volumes acquired during the entire scan. In FAIR ASL, tSNR and CNR were calculated from the subtracted CBF-weighted images.

Results

Representative CBV-weighted and CBF-weighted (after surround subtraction) images from 3D VASO-FAIR are shown in Figures 3a,b, respectively. Figures 3c,d show the corresponding images from separate VASO and FAIR-ASL scans with the same scales. The quality and contrast of the images are comparable between combined and separate scans.

The fMRI results from the combined 3D VASO-FAIR scans and separate VASO and FAIR scans are compared further in Figure 4 and Table 1. The voxels meeting activation criteria (highlighted with their t-scores) are mostly localized in the visual cortex (representative images for VASO in Figures 4a,b and for FAIR in Figures 4d,e; 16 slices acquired, 4 slices shown), and the spatial patterns of activation are similar between the combined and separate VASO and FAIR scans. A few spurious activations outside the visual regions were observed in some of the subjects, but these were excluded from further analysis as the focus of this study is to compare the separate and combined scans in the visual cortex. In the subsequent quantitative comparisons, only voxels that are activated in both separate and combined scans were used.

The time courses averaged over all slices and all subjects matched well between the separate and combined scans for both VASO (Figure 4c) and FAIR (Figure 4f). The relative signal changes (ΔS/S), tSNR and CNR per scan were all statistically comparable ($P>0.1$) between combined and separate scans for VASO and FAIR, respectively. CNR per unit time for VASO was higher in the separate scan ($P<0.01$) than in the 3D VASO-FAIR scan, as only half of VASO scans were acquired in the combined scan. CNR per unit time for FAIR was comparable ($P>0.1$) between separate and combined scans.

Relative CBV and CBF changes upon visual stimulation were quantified based on the measured VASO and FAIR ΔS/S, respectively. Using the theory and parameters from (Donahue et al., 2006a; Hua et al., 2011c; Lu et al., 2003), the relative CBV change was calculated as 37.1%±3.9% (separate scan) and 34.8%±6.3% (combined scan), whereas the relative CBF change was 38.6%±6.1% (separate scan) and 42.7% ± 8.3% (combined scan).

Discussion

We developed a 3D whole-brain imaging technique to simultaneously detect CBV and CBF responses upon functional stimulation in a single MRI scan. This is expected to be useful especially for the quantitative BOLD approaches in which concurrent CBV and CBF measurements are desired. Compared to sequentially obtaining CBV and CBF

NIH-PA Author Manuscript

NIH-PA Author Manuscript

NIH-PA Author Manuscript

measurements using individual scans, this technique will not only improve the acquisition efficiency, but also reduce potential confounding effects resulting from head motion, task performance variation and physiologic fluctuations between MRI scans. Compared with the original separate VASO and FAIR scans, the proposed approach demonstrated similar image quality, activation patterns and relative signal changes (ΔS/S) during functional stimulation, as well as comparable tSNR and CNR values per scan. The fact that ΔS/S in the separate and combined scans are consistent indicates that they are measuring the same contrast (CBV and CBF changes for VASO and FAIR, respectively). Bloch simulations demonstrated that the GM signals in the VASO and FAIR scans in the combined method are both slightly lower than those in the corresponding separate scans (VASO: 20% vs. 23%; FAIR: 57% vs. 59%). Nevertheless, tSNR and CNR per scan were all comparable between the corresponding separate and combined scans in our data (Table 1). This can be explained by the fact that physiological noise is dominant in fMRI, thus a slight loss in MR signal might not lead to a decrease in tSNR (Gonzalez-Castillo et al., 2011; Kruger and Glover, 2001; Kruger et al., 2001; Triantafyllou et al., 2005). Indeed, we found that the noise levels (calculated as the standard deviation along the time course during the baseline period) were lower in the combined scans from all six subjects.

In the proposed approach, we adopted a 3D fast GRE imaging sequence, which has much less geometric distortion and fewer signal dropouts than the traditional GRE echo-planar-imaging (EPI) sequence and is commonly used in high-resolution anatomical scans such as the Magnetization Prepared RApid Gradient Echo (MPRAGE) sequence (Hua et al., 2013b; Mugler and Brookeman, 1990; Qin et al., 2014). For VASO fMRI, this readout minimizes the BOLD contamination by allowing a very short TE (< 2ms) to be used (Hua et al., 2013a). For CBF measurement, a 3D readout can eliminate the artifactual inter-slice variation of perfusion signals originating from slice-dependent post-labeling delay times in 2D acquisition methods (Gai et al., 2011; Gunther et al., 2005). A low-high (also known as “centric”) phase encoding scheme was used in the 3D GRE readout. This means that the center of k-space (kz=ky=0 for 3D), which determines the gross signal intensity in the image, was acquired at the first echo. This is important for blood nulling in VASO (Hua et al., 2013a) and CBF quantification in ASL. Nevertheless, while the signal intensity in MRI images is dictated by the center of k-space, the evolution of magnetizations during the rest of the readout train when outer k-space lines are acquired would lead to a distorted point spread function (PSF), which causes blurring artifacts in the images (Epstein et al., 1996; Hua et al., 2013a; Lin and Bernstein, 2008). For static spins (tissue), such artifacts are shown to be minimal when a low FA (<20°) is used in 3D fast GRE with short TR (Epstein et al., 1996). For inflowing spins (blood), a recent study using a similar 3D readout demonstrates that the blurring effects are small with vascular transit times ranging from 1.1 to 2.3 s (Nielsen and Hernandez-Garcia, 2013). The PSF for the sequence used in this study was calculated, which was only slightly distorted with maximum amplitude of the side lobes less than 5% of the main peak. This indicates that such blurring artifacts are minimal in our sequence with a FA of 7° and a short TR of 3.6 ms.

In this proof-of-concept study, we chose a spatial resolution of 5mm isotropic to boost the sensitivity (SNR) of the measurements, and to demonstrate the principles of the 3D VASO-FAIR method. This may lead to significant partial-volume effects from WM in the GM

NIH-PA Author Manuscript

NIH-PA Author Manuscript

NIH-PA Author Manuscript

signals. WM is known to have much smaller CBV and CBF values, and a longer arterial transit time than GM, the change of which during a typical flashing checker board visual stimulation is known to be quite small (Leenders et al., 1990; van Gelderen et al., 2008; van Osch et al., 2009). This may bring down the overall perfusion signal changes in the large voxels measured in our data. Although this partial volume effect should not undermine the comparison between the separate and combined approaches here, for future quantitative physiological studies, finer spatial resolution, which can be achieved by adapting the readout pulse sequence and utilizing fast imaging techniques such as parallel imaging and partial Fourier sampling, may be used to alleviate this problem. Besides, a high resolution anatomical scan may be acquired for each subject in order to correct for such effects in the perfusion measurements.

CSF may also have partial volume effects with GM, which usually result in more negative VASO signal changes (Donahue et al., 2006a; Scouten and Constable, 2007, 2008). From the Bloch simulations (see Methods), the steady state CSF signals in the combined scan are less negative (−4% of the equilibrium signal) in VASO and more positive (19%) in FAIR ASL than the respective separate scans (VASO −9%, FAIR ASL 15%). Simulations also indicate that the CSF contamination in the VASO signal change is slightly smaller in the combined scan due to the less negative CSF signal, which may at least partially explain the less negative (albeit not statistically significant) ΔS/S in the combined VASO scan (Table 1). For FAIR ASL, as it is generally reasonable to assume comparable CSF signals in both label and control scans, this partial volume effect should not affect the difference signal (perfusion). The situation where CSF volume changes during activation was not simulated in this study, as it seems unclear so far whether and how much the CSF volume alters, which may need further investigation. Several techniques, such as VASO-FLAIR (Donahue et al., 2006a) and VASO ACDC (Scouten and Constable, 2007, 2008) may possibly be incorporated to suppress the CSF contamination in the VASO signals with careful design of the timing of pulse sequence.

The inflow effect in VASO MRI is suppressed by a post-saturation module in the 3D VASO-FAIR sequence. As shown in previous work (Hua et al., 2013a), the inflowing blood spins in VASO can be categorized into three different types depending on their times entering the transmit coil: I) spins flowing in before the end of readout of the previous TR; II) spins flowing in between the readout of previous TR and the inversion pulse of current TR; III) spins flowing after the inversion pulse of current TR. The post-saturation method only eliminates type I inflowing spins. Type II and III spins can be suppressed by the motion-sensitized driven equilibrium (MSDE) technique. In the current study, we did not apply MSDE in both the separate and combined scans for the following reasons: 1) The inflow effects from type II and III spins are relatively small when a body coil is used for RF transmit at 3T with a relatively long TR (Donahue et al., 2009b; Donahue et al., 2006a; Lu, 2008); 2) The main goal of this study is to compare the separate and combined scans with the same imaging parameters. However, this may result in larger VASO signal changes in our data due to residual type II and III spins, and the MSDE module (Hua et al., 2013a) should be applied in future quantitative studies.

NIH-PA Author Manuscript

NIH-PA Author Manuscript

NIH-PA Author Manuscript

Another confounding effect for CBF and CBV quantification comes from the alteration in vascular transit times upon functional stimulation. In VASO, a spatially non-selective inversion is used and the inflow effect, which is more prominent at short TR, is largely suppressed by the post-saturation module. Therefore, we expect that transit time changes upon stimulation have minor influence on the VASO signal changes with a relatively long TR used in this study. For FAIR ASL, it is well known that scans with a single post-labeling delay (TI) are more sensitive to bolus transit time changes, which is especially problematic for short TIs. With a relatively long TI used here for FAIR ASL, it has been shown that this confounding effect is quite small for typical transit time changes during functional stimulation in human brain (Alsop et al., 2014; Donahue et al., 2006b). In addition, the first readout pulse train in the 3D VASO-FAIR sequence may saturate some of the inflowing blood spins that will eventually contribute to the FAIR ASL signals acquired in the second readout. This would not affect the relative signal change in FAIR ASL if the vascular transit time does not change between baseline and activation. To evaluate the situation when the transit time does change, Bloch simulations were performed in which the signals from blood spins that reach the imaging volume after each excitation pulse in the first readout were calculated individually (because they see different numbers of excitation pulses), and the weighted sum of these blood signals (depending on transit times) was taken as the total blood signal when the FAIR ASL images are acquired in the second readout. The same imaging parameters described in Methods were used, and a baseline bolus arrival time of 400 ms with a 15% decrease upon visual stimulation (Hua et al., 2011a) was assumed. The results from simulation indicate that such a transit time effect will only increase the relative signal change in FAIR ASL with <5% as compared to a pure CBF increase. To correct for these confounding effects in CBF quantification, methods such as QUIPPS II (Luh et al., 1999; Wong et al., 1998) and/or multiple post-labeling delays can be employed (Dai et al., 2012) in future studies, especially in certain physiological conditions where transit time changes drastically.

Taking these confounding effects together, the relative changes in FAIR ASL signals and CBF during visual stimulation in our data are relatively low compared to typical literature values. We attribute this mainly to a substantial partial volume effect from WM. On the other hand, the VASO signal changes and estimated CBV changes are comparable to literature values, which may be explained by the fact that counteracting confounding effects (partial volume effects from WM decreases the VASO signal changes; but CSF contamination and residual inflow effect increase the VASO signal changes) cancel out with each other on the final VASO signal change. Note that the proposed method is designed for functional studies where relative changes in CBF and CBV are of interest. The traditional VASO approach alone cannot measure absolute baseline CBV. For ASL, while it yields signals that are linearly proportional to CBF, absolute quantification of CBF requires careful evaluation of potential confounds which we feel is beyond the scope of the current study.

Power deposition does not seem to be a major limiting factor in the combined pulse sequence used here, mainly due to the low FA in the 3D GRE readout and the relatively long TR and readout duration. The specific absorption rate (SAR) is about 1.0 W/kg (<30% of the FDA limit for head exposure) for the proposed 3D VASO-FAIR sequence with the parameters used in this study. If the MT pre-pulse is turned off (with other parameters

NIH-PA Author Manuscript

NIH-PA Author Manuscript

NIH-PA Author Manuscript

identical), SAR will decrease to about 0.3 W/kg (<9% of the FDA limit). Note that the 400 ms 2.5 μT block-shaped MT prepulse can also be replaced by a pulse train to further lower the SAR level. With the same imaging parameters used here, the 3D VASO-FAIR sequence can acquire up to 30 slices with a SAR level less than 1.1 W/kg (<34% of the FDA limit) at 3T. In this case, the actual bottleneck is the long readout pulse train for one image volume and TR, instead of power deposition.

In this first study, we chose to use the original forms of pulse sequences for FAIR ASL and VASO. Over the past decade, many improvements have been developed for these methods, including vascular crushing gradients, QUIPSS (QUIPSS II and Q2TIPS), multiple post-labeling delays, background suppression, pseudo-continuous labeling for ASL (Alsop et al., 2014), and the inflow-based VASO (iVASO) approach (Donahue et al., 2009c; Donahue et al., 2010; Hua et al., 2009b, 2011a; Hua et al., 2009c, 2011b) for VASO. We are currently working to incorporate some of these improvements into the proposed approach. For instance, crusher gradients (Le Bihan et al., 1988) or the motion-sensitized driven equilibrium (MSDE) preparation (Balu et al., 2011; Hua et al., 2013a; Wang et al., 2007; Wang et al., 2010) can be added to suppress macro-vascular signal contaminations in ASL. The combined sequence can also be adapted with the QUIPSS modifications (Luh et al., 1999; Wong et al., 1998) to control the labeling bolus width. Scans at multiple post-labeling delays (TI) (Buxton et al., 1998; Dai et al., 2012; Francis et al., 2008; Gonzalez-At et al., 2000; Gunther et al., 2001; Petersen et al., 2006; Wang et al., 2013) can be achieved by deploying multiple readout modules within one scan (TR) or using separate scans for each TI, in order to obtain direct information on vascular transit times and to reduce errors in CBF quantification due to transit time variations. However, similar to other ASL methods, this is certainly limited by factors such as TR, readout length, power deposition and total scan time. Although theoretically feasible, careful design of the timing and number of saturation and inversion pulses is needed to incorporate background suppression (Dai et al., 2008; Dixon et al., 1991; Garcia et al., 2005; Maleki et al., 2012; Ye et al., 2000) into the proposed method. FAIR ASL is a pulsed ASL (PASL) scheme. Therefore, pseudo-continuous labeling (Dai et al., 2008; Wong, 2007; Wu et al., 2007b), which generally has higher SNR than PASL, cannot be used here, which may be one of the disadvantages for the proposed method. The inversion schemes in iVASO (Donahue et al., 2009c; Donahue et al., 2010; Hua et al., 2009b, 2011a; Hua et al., 2009c, 2011b)can also be used here, which should result in enhanced SNR, and a CBV contrast dominated by the arterial compartment. Proper single TI or multiple TIs should be used to mitigate arterial transit time effects in the iVASO contrast (Donahue et al., 2009c; Donahue et al., 2010; Hua et al., 2009b, 2011a; Hua et al., 2009c, 2011b).

One drawback of the proposed 3D VASO-FAIR sequence is that the temporal resolution for the VASO scans are halved compared to the separate VASO approach, as VASO images can only be acquired at TI_1 in each NS scan but not in the SS scans where no global inversion is applied and out-of-slab blood is not properly nulled. Hence, CNR per unit time for VASO was lower in the combined method compared to the separate VASO scan (Table 1). On the other hand, since the out-of-slab blood signal is higher during the SS scans in the combined scans as compared to the blood signals in separate VASO scans, it acts as a suppressor for the CBF contamination in the VASO contrast. As a post-saturation module is already

NIH-PA Author Manuscript

NIH-PA Author Manuscript

NIH-PA Author Manuscript

applied here to suppress the flow related artifacts in VASO, this extra suppression effect is not obvious in the data. However, VASO ΔS/S in the combined scans appeared slightly lower (albeit not statistically significant) than in separate scans (Table 1), which may indicate some residual CBF contamination at TR of 3s being suppressed. This suppression effect should be more useful for VASO scans with shorter TRs in which the flow related contamination is more prominent (Donahue et al., 2009b; Lu et al., 2013).

Conclusions

A 3D perfusion imaging approach was demonstrated that combines the VASO and FAIR-ASL MRI techniques, allowing the measurement of CBV and CBF dynamics during functional stimulation in a single scan. Using a flashing checker board visual stimulation paradigm, activation patterns with signal changes (ΔS/S), tSNR and CNR per scan comparable to the original individual methods were detected. This approach is expected to provide a more efficient and equally sensitive alternative when both CBV and CBF responses need to be monitored during a functional task, such as needed for the quantitative BOLD fMRI studies where information about oxygen metabolism alterations can be extracted from the BOLD and hemodynamic measures.

Supplementary Material

Refer to Web version on PubMed Central for supplementary material.

Acknowledgments

The authors thank Mr. Joseph S. Gillen, Ms. Terri Lee Brawner and Ms. Kathleen A. Kahl for experimental assistance. This project was supported by the National Institute of Biomedical Imaging and Bioengineering of the National Institutes of Health through resource grant P41 EB015909. Equipment used in the study is manufactured by Philips. Dr. van Zijl is a paid lecturer for Philips Medical Systems. Dr. van Zijl is the inventor of technology that is licensed to Philips. This arrangement has been approved by Johns Hopkins University in accordance with its conflict of interest policies.

References

Alsop DC, Detre JA. Reduced transit-time sensitivity in noninvasive magnetic resonance imaging of human cerebral blood flow. J Cereb Blood Flow Metab. 1996; 16:1236–1249. [PubMed: 8898697]

Alsop DC, Detre JA, Golay X, Gunther M, Hendrikse J, Hernandez-Garcia L, Lu H, Macintosh BJ, Parkes LM, Smits M, van Osch MJ, Wang DJ, Wong EC, Zaharchuk G. Recommended implementation of arterial spin-labeled perfusion MRI for clinical applications: A consensus of the ISMRM perfusion study group and the European consortium for ASL in dementia. Magn Reson Med. 201410.1002/mrm.25197.

Balaban RS, Chesnick S, Hedges K, Samaha F, Heineman FW. Magnetization transfer contrast in MR imaging of the heart. Radiology. 1991; 180:671–675. [PubMed: 1871277]

Balu N, Yarnykh VL, Chu B, Wang J, Hatsukami T, Yuan C. Carotid plaque assessment using fast 3D isotropic resolution black-blood MRI. Magn Reson Med. 2011; 65:627–637. [PubMed: 20941742]

Blockley NP, Francis ST, Gowland PA. Perturbation of the BOLD response by a contrast agent and interpretation through a modified balloon model. Neuroimage. 2009; 48:84–93. [PubMed: 19559799]

Blockley NP, Griffeth VE, Simon AB, Buxton RB. A review of calibrated blood oxygenation level-dependent (BOLD) methods for the measurement of task-induced changes in brain oxygen metabolism. NMR Biomed. 2013; 26:987–1003. [PubMed: 22945365]

NIH-PA Author Manuscript NIH-PA Author Manuscript NIH-PA Author Manuscript

Brookes MJ, Morris PG, Gowland PA, Francis ST. Noninvasive measurement of arterial cerebral blood volume using Look-Locker EPI and arterial spin labeling. Magn Reson Med. 2007; 58:41–54. [PubMed: 17659615]

Buxton RB, Frank LR, Wong EC, Siewert B, Warach S, Edelman RR. A general kinetic model for quantitative perfusion imaging with arterial spin labeling. Magn Reson Med. 1998; 40:383–396. [PubMed: 9727941]

Chen JJ, Pike GB. BOLD-specific cerebral blood volume and blood flow changes during neuronal activation in humans. NMR Biomed. 2009; 22:1054–1062. [PubMed: 19598180]

Dai W, Garcia D, de Bazelaire C, Alsop DC. Continuous flow-driven inversion for arterial spin labeling using pulsed radio frequency and gradient fields. Magn Reson Med. 2008; 60:1488–1497. [PubMed: 19025913]

Dai W, Robson PM, Shankaranarayanan A, Alsop DC. Reduced resolution transit delay prescan for quantitative continuous arterial spin labeling perfusion imaging. Magn Reson Med. 2012; 67:1252–1265. [PubMed: 22084006]

Davis TL, Kwong KK, Weisskoff RM, Rosen BR. Calibrated functional MRI: mapping the dynamics of oxidative metabolism. Proc Natl Acad Sci U S A. 1998; 95:1834–1839. [PubMed: 9465103]

Dixon WT, Sardashti M, Castillo M, Stomp GP. Multiple inversion recovery reduces static tissue signal in angiograms. Magn Reson Med. 1991; 18:257–268. [PubMed: 2046511]

Donahue MJ, Blicher JU, Ostergaard L, Feinberg DA, MacIntosh BJ, Miller KL, Gunther M, Jezzard P. Cerebral blood flow, blood volume, and oxygen metabolism dynamics in human visual and motor cortex as measured by whole-brain multi-modal magnetic resonance imaging. J Cereb Blood Flow Metab. 2009a; 29:1856–1866. [PubMed: 19654592]

Donahue MJ, Hua J, Pekar JJ, van Zijl PC. Effect of inflow of fresh blood on vascular-space-occupancy (VASO) contrast. Magn Reson Med. 2009b; 61:473–480. [PubMed: 19161167]

Donahue MJ, Lu H, Jones CK, Edden RA, Pekar JJ, van Zijl PC. Theoretical and experimental investigation of the VASO contrast mechanism. Magn Reson Med. 2006a; 56:1261–1273. [PubMed: 17075857]

Donahue MJ, Lu H, Jones CK, Pekar JJ, van Zijl PC. An account of the discrepancy between MRI and PET cerebral blood flow measures. A high-field MRI investigation. NMR Biomed. 2006b; 19:1043–1054. [PubMed: 16948114]

Donahue, MJ.; MacIntosh, BJ.; Sideso, E.; Bright, M.; Kennedy, J.; Handa, A.; Jezzard, P. Absolute cerebral blood volume (CBV) quantification without contrast agents using inflow vascular-space-occupancy (iVASO) with dynamic subtraction. Proc 17th Annual Meeting ISMRM; Honolulu, Hawai'i, USA, 0628. 2009c.

Donahue MJ, Sideso E, MacIntosh BJ, Kennedy J, Handa A, Jezzard P. Absolute arterial cerebral blood volume quantification using inflow vascular-space-occupancy with dynamic subtraction magnetic resonance imaging. J Cereb Blood Flow Metab. 2010; 30:1329–1342. [PubMed: 20145656]

Donahue MJ, Stevens RD, de Boorder M, Pekar JJ, Hendrikse J, van Zijl PC. Hemodynamic changes after visual stimulation and breath holding provide evidence for an uncoupling of cerebral blood flow and volume from oxygen metabolism. J Cereb Blood Flow Metab. 2009d; 29:176–185. [PubMed: 18797471]

Epstein FH, Mugler JP 3rd, Brookeman JR. Spoiling of transverse magnetization in gradient-echo (GRE) imaging during the approach to steady state. Magn Reson Med. 1996; 35:237–245. [PubMed: 8622589]

Francis ST, Bowtell R, Gowland PA. Modeling and optimization of Look-Locker spin labeling for measuring perfusion and transit time changes in activation studies taking into account arterial blood volume. Magn Reson Med. 2008; 59:316–325. [PubMed: 18183614]

Gai ND, Talagala SL, Butman JA. Whole-brain cerebral blood flow mapping using 3D echo planar imaging and pulsed arterial tagging. J Magn Reson Imaging. 2011; 33:287–295. [PubMed: 21274969]

Garcia DM, Duhamel G, Alsop DC. Efficiency of inversion pulses for background suppressed arterial spin labeling. Magn Reson Med. 2005; 54:366–372. [PubMed: 16032674]

NIH-PA Author Manuscript NIH-PA Author Manuscript NIH-PA Author Manuscript

Gonzalez-At JB, Alsop DC, Detre JA. Cerebral perfusion and arterial transit time changes during task activation determined with continuous arterial spin labeling. Magn Reson Med. 2000; 43:739–746. [PubMed: 10800040]

Gonzalez-Castillo J, Roopchansingh V, Bandettini PA, Bodurka J. Physiological noise effects on the flip angle selection in BOLD fMRI. NeuroImage. 2011; 54:2764–2778. [PubMed: 21073963]

Grubb RL Jr, Raichle ME, Eichling JO, Ter-Pogossian MM. The effects of changes in PaCO2 on cerebral blood volume, blood flow, and vascular mean transit time. Stroke. 1974; 5:630–639. [PubMed: 4472361]

Gu H, Stein EA, Yang Y. Nonlinear responses of cerebral blood volume, blood flow and blood oxygenation signals during visual stimulation. Magn Reson Imaging. 2005; 23:921–928. [PubMed: 16310107]

Gunther M, Bock M, Schad LR. Arterial spin labeling in combination with a look-locker sampling strategy: inflow turbo-sampling EPI-FAIR (ITS-FAIR). Magn Reson Med. 2001; 46:974–984. [PubMed: 11675650]

Gunther M, Oshio K, Feinberg DA. Single-shot 3D imaging techniques improve arterial spin labeling perfusion measurements. Magn Reson Med. 2005; 54:491–498. [PubMed: 16032686]

Hoge RD, Atkinson J, Gill B, Crelier GR, Marrett S, Pike GB. Investigation of BOLD signal dependence on cerebral blood flow and oxygen consumption: the deoxyhemoglobin dilution model. Magn Reson Med. 1999; 42:849–863. [PubMed: 10542343]

Hua J, Donahue MJ, Zhao JM, Grgac K, Huang AJ, Zhou J, van Zijl PC. Magnetization transfer enhanced vascular-space-occupancy (MT-VASO) functional MRI. Magn Reson Med. 2009a; 61:944–951. [PubMed: 19215043]

Hua J, Jones CK, Qin Q, van Zijl PC. Implementation of vascular-space-occupancy MRI at 7T. Magn Reson Med. 2013a; 69:1003–1013. [PubMed: 22585570]

Hua, J.; Qin, Q.; Donahue, MJ.; Zhou, J.; Pekar, JJ.; van Zijl, PC. Functional MRI using arteriolar cerebral blood volume changes. Proc 17th Annual Meeting ISMRM; Honolulu, Hawai'i, USA, 0012. 2009b.

Hua J, Qin Q, Donahue MJ, Zhou J, Pekar JJ, van Zijl PC. Inflow-based vascular-space-occupancy (iVASO) MRI. Magn Reson Med. 2011a; 66:40–56. [PubMed: 21695719]

Hua, J.; Qin, Q.; Pekar, JJ.; van Zijl, PC. Measuring absolute arteriolar cerebral blood volume (CBVa) in human brain gray matter (GM) without contrast agent. Proc 17th Annual Meeting ISMRM; Honolulu, Hawai'i, USA, 1533. 2009c.

Hua J, Qin Q, Pekar JJ, van Zijl PC. Measurement of absolute arterial cerebral blood volume in human brain without using a contrast agent. NMR Biomed. 2011b; 24:1313–1325. [PubMed: 21608057]

Hua J, Qin Q, van Zijl PC, Pekar JJ, Jones CK. Whole-brain three-dimensional T2-weighted BOLD functional magnetic resonance imaging at 7 Tesla. Magn Reson Med. 2013b10.1002/mrm.25055.

Hua, J.; Stevens, RD.; Donahue, MJ.; Huang, AJ.; Pekar, JJ.; van Zijl, PC. Cerebral blood volume changes in arterial and post-arterial compartments and their relationship with cerebral blood flow alteration during brief breath-holding and visual stimulation in human brain. Proc 18th Annual Meeting ISMRM; Stockholm, Sweden. 2010. p. 2749

Hua J, Stevens RD, Huang AJ, Pekar JJ, van Zijl PC. Physiological origin for the BOLD poststimulus undershoot in human brain: vascular compliance versus oxygen metabolism. J Cereb Blood Flow Metab. 2011c; 31:1599–1611. [PubMed: 21468090]

Huber L, Ivanov D, Krieger SN, Streicher MN, Mildner T, Poser BA, Moller HE, Turner R. Slab-selective, BOLD-corrected VASO at 7 tesla provides measures of cerebral blood volume reactivity with high signal-to-noise ratio. Magn Reson Med. 201310.1002/mrm.24916.

Ito H, Takahashi K, Hatazawa J, Kim SG, Kanno I. Changes in human regional cerebral blood flow and cerebral blood volume during visual stimulation measured by positron emission tomography. J Cereb Blood Flow Metab. 2001; 21:608–612. [PubMed: 11333371]

Kim SG. Quantification of relative cerebral blood flow change by flow-sensitive alternating inversion recovery (FAIR) technique: application to functional mapping. Magn Reson Med. 1995; 34:293–301. [PubMed: 7500865]

NIH-PA Author Manuscript NIH-PA Author Manuscript NIH-PA Author Manuscript

Krieger, SN.; Huber, L.; Egan, G.; Turner, R. Simultaneous acquisition of cerebral blood volume, blood flow and blood oxygenation weighted MRI signals at 7T. Proc 21st Annual Meeting ISMRM; Salt Lake City, Utah, USA, 0107. 2013.

Kruger G, Glover GH. Physiological noise in oxygenation-sensitive magnetic resonance imaging. Magn Reson Med. 2001; 46:631–637. [PubMed: 11590638]

Kruger G, Kastrup A, Glover GH. Neuroimaging at 1.5 T and 3.0 T: comparison of oxygenation-sensitive magnetic resonance imaging. Magn Reson Med. 2001; 45:595–604. [PubMed: 11283987]

Kwong KK, Chesler DA, Weisskoff RM, Donahue KM, Davis TL, Ostergaard L, Campbell TA, Rosen BR. MR perfusion studies with T1-weighted echo planar imaging. Magn Reson Med. 1995; 34:878–887. [PubMed: 8598815]

Le Bihan D, Breton E, Lallemand D, Aubin ML, Vignaud J, Laval-Jeantet M. Separation of diffusion and perfusion in intravoxel incoherent motion MR imaging. Radiology. 1988; 168:497–505. [PubMed: 3393671]

Leenders KL, Perani D, Lammertsma AA, Heather JD, Buckingham P, Healy MJ, Gibbs JM, Wise RJ, Hatazawa J, Herold S, et al. Cerebral blood flow, blood volume and oxygen utilization. Normal values and effect of age. Brain. 1990; 113 (Pt 1):27–47. [PubMed: 2302536]

Lin AL, Fox PT, Yang Y, Lu H, Tan LH, Gao JH. Evaluation of MRI models in the measurement of CMRO2 and its relationship with CBF. Magn Reson Med. 2008; 60:380–389. [PubMed: 18666102]

Lin AL, Fox PT, Yang Y, Lu H, Tan LH, Gao JH. Time-dependent correlation of cerebral blood flow with oxygen metabolism in activated human visual cortex as measured by fMRI. Neuroimage. 2009; 44:16–22. [PubMed: 18804541]

Lin AL, Lu H, Fox PT, Duong TQ. Cerebral Blood Volume Measurements - Gd_DTPA vs. VASO - and Their Relationship with Cerebral Blood Flow in Activated Human Visual Cortex. Open Neuroimag J. 2011; 5:90–95. [PubMed: 22253653]

Lin C, Bernstein MA. 3D magnetization prepared elliptical centric fast gradient echo imaging. Magn Reson Med. 2008; 59:434–439. [PubMed: 18183604]

Lu, H. Magnetization “reset” for non-steady-state blood spins in Vascular-Space-Occupancy (VASO) fMRI. Proc 16th Annual Meeting ISMRM; Toronto, Canada. 2008. p. 406

Lu H, Clingman C, Golay X, van Zijl PC. Determining the longitudinal relaxation time (T1) of blood at 3.0 Tesla. Magn Reson Med. 2004a; 52:679–682. [PubMed: 15334591]

Lu H, Donahue MJ, van Zijl PC. Detrimental effects of BOLD signal in arterial spin labeling fMRI at high field strength. Magn Reson Med. 2006; 56:546–552. [PubMed: 16894581]

Lu H, Golay X, Pekar JJ, Van Zijl PC. Functional magnetic resonance imaging based on changes in vascular space occupancy. Magn Reson Med. 2003; 50:263–274. [PubMed: 12876702]

Lu H, Golay X, Pekar JJ, Van Zijl PC. Sustained poststimulus elevation in cerebral oxygen utilization after vascular recovery. J Cereb Blood Flow Metab. 2004b; 24:764–770. [PubMed: 15241184]

Lu H, Hua J, van Zijl PC. Noninvasive functional imaging of cerebral blood volume with vascular-space-occupancy (VASO) MRI. NMR Biomed. 2013; 26:932–948. [PubMed: 23355392]

Lu H, Nagae-Poetscher LM, Golay X, Lin D, Pomper M, van Zijl PC. Routine clinical brain MRI sequences for use at 3.0 Tesla. J Magn Reson Imaging. 2005; 22:13–22. [PubMed: 15971174]

Luh WM, Wong EC, Bandettini PA, Hyde JS. QUIPSS II with thin-slice TI1 periodic saturation: a method for improving accuracy of quantitative perfusion imaging using pulsed arterial spin labeling. Magn Reson Med. 1999; 41:1246–1254. [PubMed: 10371458]

Maleki N, Dai W, Alsop DC. Optimization of background suppression for arterial spin labeling perfusion imaging. MAGMA. 2012; 25:127–133. [PubMed: 22009131]

Mugler JP 3rd, Brookeman JR. Three-dimensional magnetization-prepared rapid gradient-echo imaging (3D MP RAGE). Magn Reson Med. 1990; 15:152–157. [PubMed: 2374495]

Nielsen JF, Hernandez-Garcia L. Functional perfusion imaging using pseudocontinuous arterial spin labeling with low-flip-angle segmented 3D spiral readouts. Magn Reson Med. 2013; 69:382–390. [PubMed: 22488451]

NIH-PA Author Manuscript NIH-PA Author Manuscript NIH-PA Author Manuscript

Ordidge RJ, Wylezinska M, Hugg JW, Butterworth E, Franconi F. Frequency offset corrected inversion (FOCI) pulses for use in localized spectroscopy. Magn Reson Med. 1996; 36:562–566. [PubMed: 8892208]

Petersen ET, Lim T, Golay X. Model-free arterial spin labeling quantification approach for perfusion MRI. Magn Reson Med. 2006; 55:219–232. [PubMed: 16416430]

Qin Q, Huang AJ, Hua J, Desmond JE, Stevens RD, van Zijl PC. Three-dimensional whole-brain perfusion quantification using pseudo-continuous arterial spin labeling MRI at multiple post-labeling delays: accounting for both arterial transit time and impulse response function. NMR Biomed. 2014; 27:116–128. [PubMed: 24307572]

Rostrup E, Knudsen GM, Law I, Holm S, Larsson HB, Paulson OB. The relationship between cerebral blood flow and volume in humans. Neuroimage. 2005; 24:1–11. [PubMed: 15588591]

Scouten A, Constable RT. Applications and limitations of whole-brain MAGIC VASO functional imaging. Magn Reson Med. 2007; 58:306–315. [PubMed: 17654574]

Scouten A, Constable RT. VASO-based calculations of CBV change: accounting for the dynamic CSF volume. Magn Reson Med. 2008; 59:308–315. [PubMed: 18228581]

Silva AC, Williams DS, Koretsky AP. Evidence for the exchange of arterial spin-labeled water with tissue water in rat brain from diffusion-sensitized measurements of perfusion. Magn Reson Med. 1997; 38:232–237. [PubMed: 9256102]

Thomas DL, Lythgoe MF, Calamante F, Gadian DG, Ordidge RJ. Simultaneous noninvasive measurement of CBF and CBV using double-echo FAIR (DEFAIR). Magn Reson Med. 2001; 45:853–863. [PubMed: 11323812]

Triantafyllou C, Hoge RD, Krueger G, Wiggins CJ, Potthast A, Wiggins GC, Wald LL. Comparison of physiological noise at 1.5 T, 3 T and 7 T and optimization of fMRI acquisition parameters. NeuroImage. 2005; 26:243–250. [PubMed: 15862224]

Uh J, Lin AL, Lee K, Liu P, Fox P, Lu H. Validation of VASO cerebral blood volume measurement with positron emission tomography. Magn Reson Med. 2011; 65:744–749. [PubMed: 21337407]

van Gelderen P, de Zwart JA, Duyn JH. Pittfalls of MRI measurement of white matter perfusion based on arterial spin labeling. Magn Reson Med. 2008; 59:788–795. [PubMed: 18383289]

van Osch MJ, Teeuwisse WM, van Walderveen MA, Hendrikse J, Kies DA, van Buchem MA. Can arterial spin labeling detect white matter perfusion signal? Magn Reson Med. 2009; 62:165–173. [PubMed: 19365865]

Wang DJ, Alger JR, Qiao JX, Gunther M, Pope WB, Saver JL, Salamon N, Liebeskind DS, Investigators US. Multi-delay multi-parametric arterial spin-labeled perfusion MRI in acute ischemic stroke - Comparison with dynamic susceptibility contrast enhanced perfusion imaging. Neuroimage Clin. 2013; 3:1–7. [PubMed: 24159561]

Wang J, Yarnykh VL, Hatsukami T, Chu B, Balu N, Yuan C. Improved suppression of plaque-mimicking artifacts in black-blood carotid atherosclerosis imaging using a multislice motion-sensitized driven-equilibrium (MSDE) turbo spin-echo (TSE) sequence. Magn Reson Med. 2007; 58:973–981. [PubMed: 17969103]

Wang J, Yarnykh VL, Yuan C. Enhanced image quality in black-blood MRI using the improved motion-sensitized driven-equilibrium (iMSDE) sequence. J Magn Reson Imaging. 2010; 31:1256–1263. [PubMed: 20432365]

Wolff SD, Balaban RS. Magnetization transfer contrast (MTC) and tissue water proton relaxation in vivo. Magn Reson Med. 1989; 10:135–144. [PubMed: 2547135]

Wong EC. Vessel-encoded arterial spin-labeling using pseudocontinuous tagging. Magn Reson Med. 2007; 58:1086–1091. [PubMed: 17969084]

Wong EC, Buxton RB, Frank LR. Quantitative imaging of perfusion using a single subtraction (QUIPSS and QUIPSS II). Magn Reson Med. 1998; 39:702–708. [PubMed: 9581600]

Wu WC, Buxton RB, Wong EC. Vascular space occupancy weighted imaging with control of residual blood signal and higher contrast-to-noise ratio. IEEE Trans Med Imaging. 2007a; 26:1319–1327. [PubMed: 17948723]

Wu WC, Fernandez-Seara M, Detre JA, Wehrli FW, Wang J. A theoretical and experimental investigation of the tagging efficiency of pseudocontinuous arterial spin labeling. Magn Reson Med. 2007b; 58:1020–1027. [PubMed: 17969096]

NIH-PA Author Manuscript

NIH-PA Author Manuscript

NIH-PA Author Manuscript

Yang Y, Gu H, Stein EA. Simultaneous MRI acquisition of blood volume, blood flow, and blood oxygenation information during brain activation. Magn Reson Med. 2004; 52:1407–1417. [PubMed: 15562477]

Ye FQ, Frank JA, Weinberger DR, McLaughlin AC. Noise reduction in 3D perfusion imaging by attenuating the static signal in arterial spin tagging (ASSIST). Magn Reson Med. 2000; 44:92–100. [PubMed: 10893526]

Ye FQ, Mattay VS, Jezzard P, Frank JA, Weinberger DR, McLaughlin AC. Correction for vascular artifacts in cerebral blood flow values measured by using arterial spin tagging techniques. Magn Reson Med. 1997; 37:226–235. [PubMed: 9001147]

Zhao JM, Clingman CS, Narvainen MJ, Kauppinen RA, van Zijl PC. Oxygenation and hematocrit dependence of transverse relaxation rates of blood at 3T. Magn Reson Med. 2007; 58:592–597. [PubMed: 17763354]

NIH-PA Author Manuscript

NIH-PA Author Manuscript

NIH-PA Author Manuscript

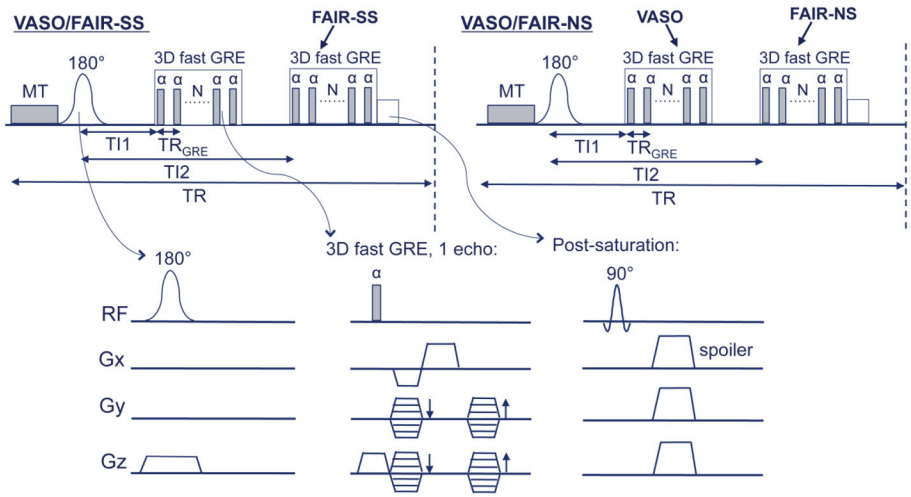

Figure 1.

Pulse sequence of the combined 3D VASO-FAIR approach. A pair of interleaving slice-selective (SS) and nonselective (NS) scans are shown. A magnetization transfer (MT) prepulse is added before the adiabatic FOCI inversion pulses. The imaging module used here is a 3D fast GRE readout for both VASO and FAIR ASL images, in which VASO signal is acquired at blood nulling time TI_1 and ASL signal at time TI_2. A post-saturation module comprising of a non-selective 90° saturation pulse and spoiler gradients is applied immediately after the FAIR ASL readout.

NIH-PA Author Manuscript
NIH-PA Author Manuscript
NIH-PA Author Manuscript

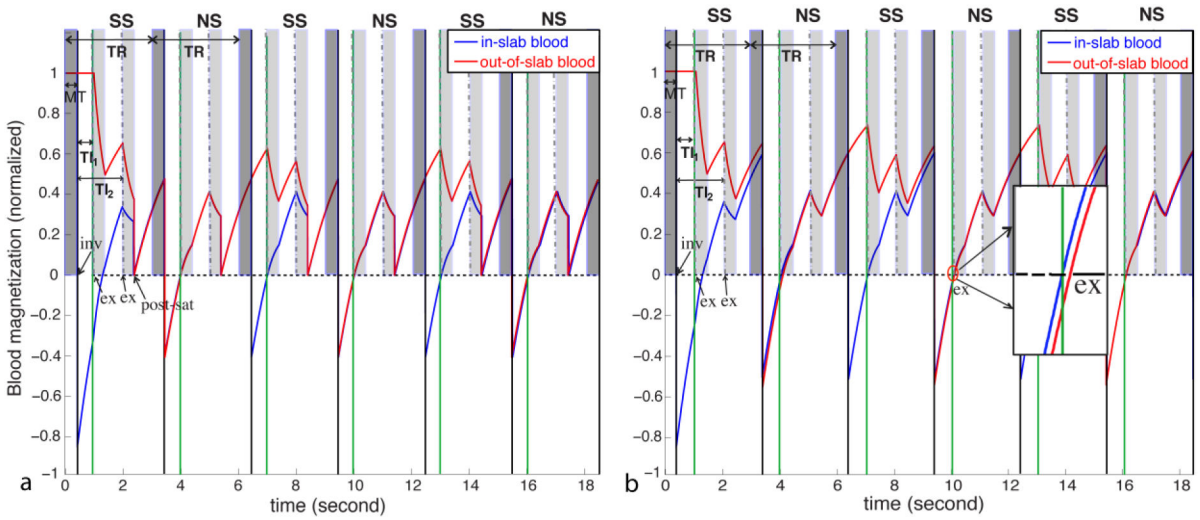

Figure 2.

Bloch simulations of the signal evolution for blood in (blue) and outside (red) the inversion slab applied in the slice-selective (SS) scan with (a) and without (b) the post-saturation module. The solid vertical black lines indicate the inversion pulses (labeled as “inv”) in the interleaving slice-selective (SS) and non-selective (NS) scans. The short dashed vertical lines represent the first excitation pulses (labeled as “ex”) in each image acquisition module, the durations of which are labeled in light shade. The MT period before the inversion pulse is labeled in dark shade. Steady state blood nulling time for VASO is marked as TI_1 (solid vertical green lines) and the post-labeling delay for FAIR as TI_2. (a) With the post-saturation module (labeled as “post-sat”) applied immediately after the second readout, a steady state is built after the first TR, at which both blood in and outside the SS inversion slab is nulled at TI_1 in the NS scan. (b) When the post-saturation module is not applied, it takes three TRs for both in-slab and out-of-slab blood to reach steady state (for the experimental parameters used) and the out-of-slab blood is not properly nulled even at steady state (zoomed inlet).

NIH-PA Author Manuscript
NIH-PA Author Manuscript
NIH-PA Author Manuscript

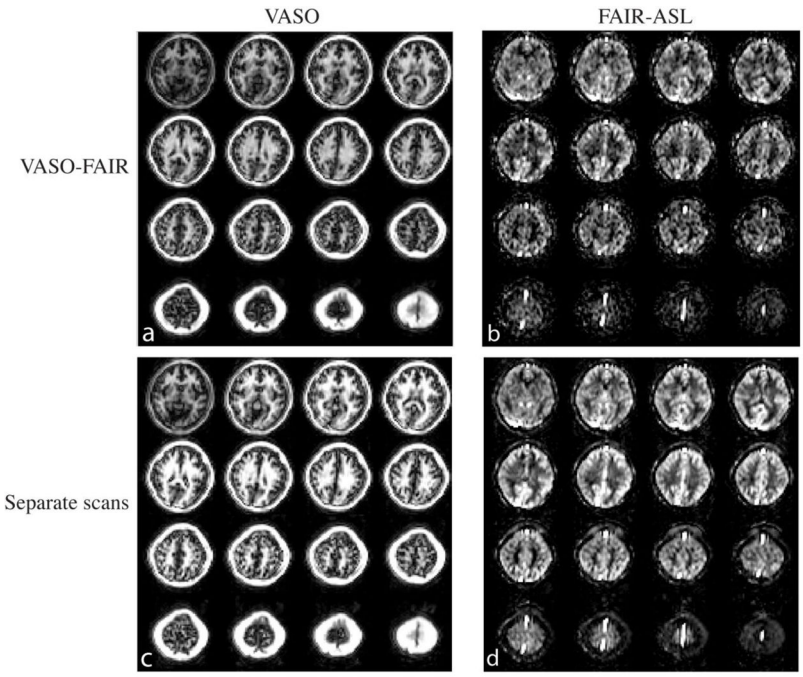

Figure 3.

Representative images from one subject. (a) Typical VASO images (3D fast GRE readout, 16 slices) from the 3D VASO-FAIR sequence. (b) Typical FAIR ASL difference maps (perfusion weighted images) in 3D VASO-FAIR. (c) Corresponding VASO images in the separate VASO scan. (d) Corresponding perfusion weighted images in the separate FAIR ASL scan. Images in (a) and (c), and (b) and (d) are on the same scales, respectively.

NIH-PA Author Manuscript

NIH-PA Author Manuscript

NIH-PA Author Manuscript

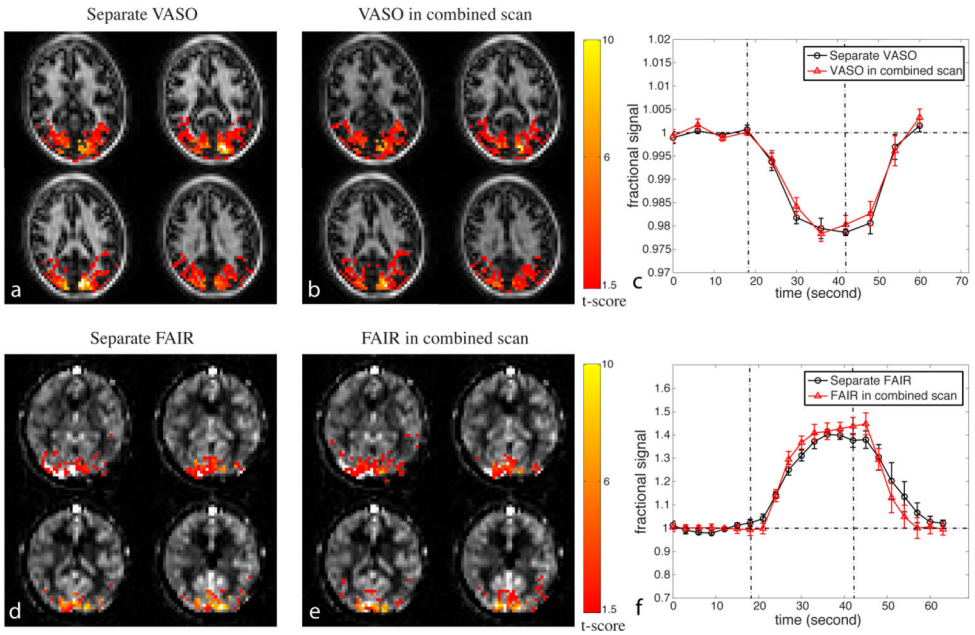

Figure 4.

Comparison of functional MRI results between the combined and separate scans. Representative activation maps from one subject for (a) separate VASO scan, (b) VASO in the combined 3D VASO-FAIR method; (d) separate FAIR ASL scan, and (e) FAIR ASL in the 3D VASO-FAIR scan are shown. The activated voxels are highlighted with their t-scores. Time courses averaged over common voxels activated in both separate (black circle) and combined (red triangle) scans (averaged over subjects, n = 6) for VASO and FAIR are shown in (c) and (f), respectively. Error bars represent inter-subject variations. The vertical dotted lines indicate the start and end of visual stimulation. Four blocks of baseline and stimulation periods were averaged to one block.

NIH-PA Author Manuscript

NIH-PA Author Manuscript

NIH-PA Author Manuscript

Table 1

Summary of quantitative fMRI results from all subjects (n = 6)

	Separate VASO	VASO in combined VASO-FAIR scan	Separate FAIR	FAIR in combined VASO-FAIR scan
ΔS/S (%)	−1.98±0.36	−1.86±0.45	38.6±6.1	42.7±8.3
tSNR	63.7±8.0	61.9±7.0	5.8±0.3	5.2±0.3
CNR per scan	1.26±0.20	1.14±0.21	2.24±0.27	2.23±0.39
CNR per unit time	12.8±2.1	8.2±1.5	22.6±2.7	22.5±3.9

Mean values ± standard deviation over all subjects. ΔS/S, tSNR and CNR were calculated as defined in Methods. Only common voxels activated in both separate and combined VASO or FAIR scans were included. All FAIR ASL results were calculated from the subtracted images (difference maps or perfusion weighted images).